

## The SABRE experiment

A. Zani\*

*INFN Milano, Via Celoria 16, 20133 Milano, Italy*

\* *andrea.zani@mi.infn.it*

D. D'Angelo

*Physics Department, University of Milan, Milan, Italy*  
*INFN Milano, Via Celoria 16, 20133 Milano, Italy*

C. Vignoli, G. Di Carlo, A. Di Giacinto, A. Ianni  
and D. Orlandi

*INFN LNGS — Laboratori Nazionali del Gran Sasso,  
67100 Assergi (L'Aquila), Italy*

A. Mariani

*Physics Department, Princeton University,  
Princeton, NJ08544, USA*

*INFN LNGS — Laboratori Nazionali del Gran Sasso,  
67100 Assergi (L'Aquila), Italy*

S. Copello†

*Physics Department, University of Genova, Genova, Italy*  
*INFN Genova, Via Dodecaneso 33, 16146 Genova, Italy*

C. Tomei, I. Dafinei, G. D'Imperio, M. Diemoz,  
M. Iannone, S. Milana and V. Pettinacci

*INFN Roma, Piazzale Aldo Moro 2, 00185 Roma, Italy*

S. Rahatlou

*Physics Department, Sapienza Università di Roma,  
Roma I-00185, Italy*

*INFN Roma, Piazzale Aldo Moro 2, 00185 Roma, Italy*

\* Corresponding author.

† Current address: Physics Department, University of Genova, Genova, Italy and INFN Genova, Via Dodecaneso 33, 16146 Genova, Italy.

F. Calaprice, A. Di Ludovico, W. Peloso,<sup>‡</sup> L. Pietrofaccia,  
M. Souza, B. Suerfu<sup>§</sup> and M. Wada<sup>¶</sup>

*Physics Department, Princeton University,  
Princeton, NJ 08544, USA*

J. Benziger

*Chemical Engineering Department, Princeton University,  
Princeton, NJ 08544, USA*

Received 31 March 2021

Accepted 12 December 2021

Published 12 April 2022

The dark matter interpretation of the DAMA/LIBRA annual modulation signal represents a long-standing open question in astroparticle physics. The SABRE experiment aims to test such claim, bringing the same detection technique to an unprecedented sensitivity. Based on ultra-low background NaI(Tl) scintillating crystals like DAMA, SABRE features a liquid scintillator Veto system, surrounding the main target, and it will deploy twin detectors: one in the Northern hemisphere at Laboratori Nazionali del Gran Sasso (LNGS), Italy and the other in the Stawell Underground Physics Laboratory (SUPL), Australia, first laboratory of this kind in the Southern hemisphere. The first very-high-purity crystal produced by the collaboration was shipped to LNGS in 2019 for characterization. It features a potassium contamination, measured by mass spectroscopy, of the order of 4 ppb, about three times lower than DAMA/LIBRA crystals. The first phase of the SABRE experiment is a Proof-of-Principle (PoP) detector featuring one crystal and a liquid scintillator Veto, at LNGS. This contribution will present the results of the stand-alone characterization of the first SABRE high-purity crystal, as well as the status of the PoP detector, commissioned early in the summer of 2020.

*Keywords:* Dark matter; annual modulation; scintillating crystals; NaI(Tl).

PACS numbers: 95.35.+d, 95.30.Cq, 29.40.Mc, 95.55.Vj, 29.40.-n

## 1. Dark Matter Search via Interaction Rate Modulation

The long-standing search for Dark Matter (DM) has produced since its beginnings many theories and candidates. Among the most sound proposals<sup>1</sup> lies the class of Weakly Interacting Massive Particles (WIMPs).<sup>2</sup> These are expected to be distributed in halos surrounding the visible matter cores of galaxies. The most common hypothesis is that WIMPs might interact via elastic scattering off target nuclei, with a resulting very small recoil energy (up to 50 keV), given their expected mass ranging from 10 GeV to few TeV. Due to the nature of the interaction, very low rates are estimated, from  $10^{-1}$  to  $10^{-6}$  events/kg/day; furthermore, such rate is

<sup>‡</sup>Current address: University of Colorado Boulder, Boulder, CO 80309, USA.

<sup>§</sup>Current address: Department of Physics, University of California, Berkeley, CA 94720, USA.

<sup>¶</sup>Current address: Nicolaus Copernicus Astronomical Center, Polish Academy of Sciences, 00716 Warszawa, Poland.

theorized to be modulated in time, with an annual sinusoidal behavior that results from the relative motion of Earth around the Sun and through the supposed DM Halo surrounding the visible counterpart of our galaxy.<sup>3</sup> The characteristics of the interaction yield the need for: (i) extremely radio-pure materials and very low background environments and (ii) an underground location, for cosmic ray shielding; the modulation, however, represents a unique signature for discovery potential.

The history of DM searches, including different techniques and target materials, reports so far only one surviving positive observation, by the DAMA Collaboration.<sup>a,4</sup> They report an annual modulation signal in the interaction rate, which satisfies the criteria for a model-independent WIMP-induced signal,<sup>3</sup> and indeed the collaboration obtained a large statistical significance of  $12.9\sigma$ ,<sup>5</sup> through over 20 years of data-taking at the Laboratori Nazionali del Gran Sasso (LNGS), Italy.

Presently, no other surviving positive observation stands, independently of the target and the detected signature (light, charge, heat), and despite the exploitation of larger target masses and lower backgrounds.<sup>6–9</sup> This implies difficulties in reconciling the DAMA results with the simplest spin-independent WIMP-nucleon elastic scattering scenarios.

### 1.1. *The need for independent verification*

An independent verification of DAMA with the same NaI(Tl) target is mandatory; however currently running NaI(Tl) DM experiments COSINE-100<sup>10</sup> (YangYang Laboratory, South Korea) and ANAIS-112<sup>11</sup> (Canfranc Laboratory, Spain) may not be sensitive enough to fully cover the DAMA allowed regions for WIMPs. Both detectors feature a mass of around 100 kg of NaI(Tl) scintillating crystals and an underground location, however this is not enough due to intrinsic backgrounds, i.e. radio-impurities from the crystals themselves. Both COSINE<sup>12</sup> and ANAIS<sup>13</sup> only ever obtained background levels (combination of intrinsic and environmental) three-four times higher than those of DAMA.

In this respect, DAMA has reached an unmatched background rate of 0.72 count/day/kg/keV in the modulation signal energy range: 1–6 keV. This should be compared with an observed modulation magnitude of 0.01 count/day/kg/keV. However, to fully constrain the WIMP phase space, it is necessary to further reduce the background and lower the energy threshold, as different modulation models start differing below the energy range indicated by DAMA. These should then be the goals of any new NaI(Tl)-based experiment aiming to fully test the DAMA results.

## 2. The SABRE Experiment

SABRE ambitious goal is to further reduce the already low background rate in the energy region of interest (ROI), as defined by DAMA, down to

<sup>a</sup>Short for DAMA/NaI and DAMA/LIBRA.

0.1 count/day/kg/keV. This challenging goal is achievable through a multi-prong approach<sup>14</sup>:

- the development of ultra-high purity NaI(Tl) crystals, starting with high-purity NaI powder and developing custom clean crystal-growth procedures;
- the achievement of very low energy threshold. This can be obtained by careful selection and employment of high Quantum Efficiency (QE) PhotoMultiplier Tubes (PMTs) directly coupled to the crystal;
- the employment of passive and active shielding (Veto detector);
- the deployment of two stations, identical in concept, in opposite hemispheres, for direct comparison of the results.

The realization of the first three points will allow reducing significantly the total detector background, effectively increasing the relative amplitude of a real modulation signal. The use of twin detectors in opposite hemispheres will allow disentangling a real DM modulation signal, expected to have the same phase everywhere on Earth, from seasonal backgrounds.

## 2.1. *High purity crystals*

The first and foremost characteristic of SABRE is the production of ultra-pure NaI(Tl) crystals with unprecedentedly low radio-contamination. Presently, the crystal growth procedure in use is the one developed by the Princeton University (PU) and Radiation Monitoring Devices (RMD) company, Boston<sup>14</sup>: it employs low-contamination Astro Grade NaI powder produced by Sigma Aldrich and vertical Bridgman–Stockbarger growth technique, sealing the powder within an ampoule that prevents contamination during the process. The aim is to produce  $\varnothing 4'' \times 8''$  long crystals, with a target mass of around 5 kg. So far, two slightly smaller crystals were produced, featuring an octagonal parallelepiped shape and mass  $\gtrsim 3$  kg.

The first crystal, called NaI-31, was grown in an RMD crucible and had a final mass (after cutting and polishing) of around 3 kg. The potassium concentration,  $[^{nat}K]$ , of Astro Grade powder is consistently measured to be lower than 10 ppb,<sup>14</sup> whereas a measurement performed on the grown crystal with Inductively Coupled Plasma Mass Spectroscopy (ICP-MS) yields a contamination of around 16 ppb, which leads to assume impurities were introduced in the growth process. The crystal was grown in Summer 2018 and later shipped by plane to LNGS in spring 2019.

A second crystal, NaI-33, was later grown in a PU crucible in Fall 2018, with a final mass of 3.4 kg. This time, ICP-MS measurements yielded a record  $[^{nat}K] \simeq 4$  ppb (see Fig. 1), around three times lower than DAMA best results. Given the exceptional result, this crystal was shipped to LNGS via boat, to minimize cosmogenic activation, arriving at LNGS in August 2019.

In order to maximize light collection, crystal bases are directly coupled with high-QE 3'' PMTs, while their lateral area is wrapped in thin layers of

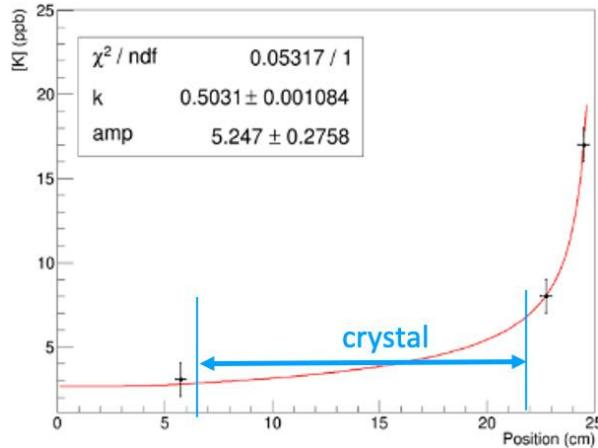


Fig. 1. Fit of the natural potassium concentration [ $^{nat}\text{K}$ ] of crystal NaI-33, derived from ICP-MS measurements on the crystal tip, tail and far-end tail.

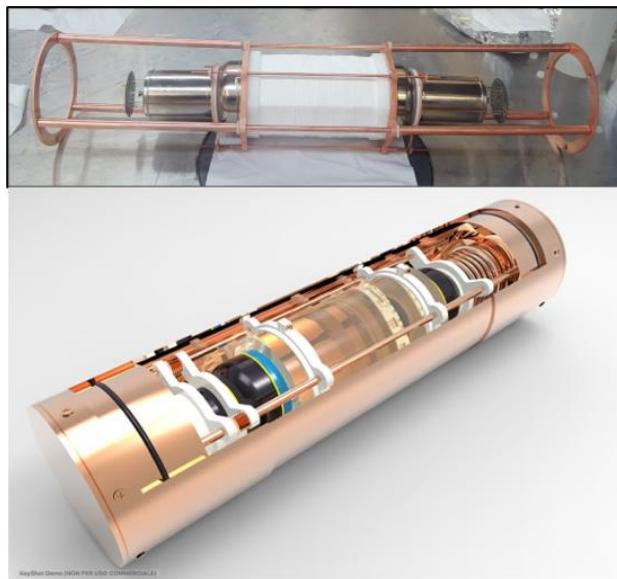


Fig. 2. Top: crystal-PMT assembly (see description in text). Bottom: render of the complete Cu-enclosure. Assuming to use multiple crystals, each one will be housed in a dedicated enclosure.

Polytetrafluoroethylene (PTFE), which works as diffusive reflector. The support structure of the crystal-PMTs assembly, as well as its container (called *Cu-enclosure*), are made of high-purity OFHC Copper, see Fig. 2.

## 2.2. Active and passive shielding

SABRE strategy is to employ both passive and active shielding. The main detector vessel is surrounded by multiple layers of materials, which are required to intercept environmental backgrounds from the underground laboratory.

Active shielding can be obtained by surrounding the main detector with a volume filled of scintillating material, mainly used to detect events escaping the crystals

region. This *Veto* volume also intercepts both environmental and intrinsic backgrounds, and it is meant to be operated with a detection threshold of the order of 100 keV. For example, among the most important intrinsic backgrounds is the decay of  $^{40}\text{K}$ : this has a 10% probability to decay via *Electron Capture* (EC), followed by an X-ray or Auger electron at 3.2 keV and a  $\gamma$ -emission of 1460 keV. The Auger electron falls exactly in the modulation signal ROI, as determined by DAMA, and therefore it could be misinterpreted as a DM event, unless a coincident detection of the  $\gamma$  in the Veto volume is recorded. Other intrinsic backgrounds that could be partially reduced by the presence of a Veto are  $^{22}\text{Na}$  and elements from the chains of  $^{232}\text{Th}$  and  $^{238}\text{U}$ , as detailed in Ref. 15.

### 2.3. Twin-station approach

The unique trait of the SABRE concept is the exploitation of two stations deployed in opposite hemispheres of the globe, in Italy and Australia. Under the assumptions of the standard halo model,<sup>17</sup> one expects a modulated Earth-Halo velocity composition, resulting in a modulated WIMP interaction rate, along the year. The use of two opposite locations should help identifying any possible contribution to the modulation due to seasonal or site-related effects. Detectors in opposite positions will obtain identical annual modulation profiles, with the same phase, if the modulation is indeed due to the DM halo. On the other hand, any modulation induced by Earth/atmospheric phenomena will be characterized by different phases. This contribution focuses on the activities of the Italian site, and the results obtained with different set-ups taking data at LNGS.

#### 2.3.1. SABRE South

The Southern hemisphere SABRE detector is being developed by the Australian components of the Collaboration and it will be hosted in the Stawell Underground Physics Laboratory (SUPL). This is a converted section of an active gold mine, in Stawell, Victoria, Australia ( $\sim 240$  km from Melbourne). Laboratory construction started in 2019, with an excavation program that was partially delayed by the outbreak of the COVID-19 pandemic in 2020. The laboratory and detector will be at a depth of 1025 m ( $\sim 2900$  m.w.e.<sup>b</sup>), a similar condition to LNGS.

Though based on the same concept detailed in Ref. 14, the SABRE-South detector has its unique features, mainly concerning the Veto: its vessel is going to be different in shape, and the chosen liquid scintillator will be based on linear alkyl benzene (LAB), whereas SABRE North has elected to use PPO-doped PseudoCumene (PC, see details in Sec. 4). LAB compatibility with the Veto materials it will be in contact with is presently under verification. At the same time, purification procedures are being defined. The main stainless steel (SS) detector vessel was constructed and delivered in 2020. Since then, the feasibility of the installation of

<sup>b</sup>m.w.e.: meter water equivalent.

components such as PMTs and Lumirror™ reflecting panels on the inner walls was heavily tested. Leak tightness tests were carried out, and cleaning/filling procedures were exercised with water. PMT readout and characterization is being performed on test-benches, with a Python-based Data AQuisition (DAQ) and analysis code.

### 3. SABRE North — Crystals Characterization

SABRE North encompasses various activities carried out at LNGS, Italy. On one side, in Hall B, a dedicated set-up is used to perform direct crystal characterization; on the other, Hall C hosts the *Proof-of-Principle* (PoP) detector, that was commissioned in summer 2020.

#### 3.1. Crystal NaI-33

LNGS Hall B hosts a dedicated set-up for single crystal testing, that is basically made of passive shielding layers, low-radioactivity copper and lead, used to intercept environmental  $\gamma$ 's. The shielding is then enclosed in a sealed plexiglass box that can be flushed with high-purity N<sub>2</sub> for Radon abatement.

The set-up allows testing a full crystal enclosure, with the same electronics chain and DAQ employed for the PoP. It was used to characterize both NaI-31 and NaI-33 crystals, the second of which underwent extensive data-taking. This set-up also represents the perfect test-bench for the optimization of data reconstruction and analysis tools, based on C++ code. The analysis allows defining background-rejection cuts, through the use of calibration sources and background runs; the crystal background model is under study as well.

Two main runs were performed with this set-up for crystal NaI-33:

- **Run1:** 08/2019–02/2020 → base shielding (5 cm Cu, 17.5 cm Pb);
- **Run2:** 02/2020–04/2020 → enhanced shielding (10 cm Cu, 17.5 cm Pb), N<sub>2</sub> flushing.

NaI-33 characterization is the focus of a dedicated paper,<sup>16</sup> therefore only some highlights will be reported here. The Light Yield (LY) and energy resolution were measured during Run1 by means of a <sup>241</sup>Am source, positioned to the side of the Cu-enclosure and aligned with the crystal centre. Obtained Light Yield for 59.5 keV photons emitted by Americium is evaluated in  $11.1 \pm 0.2$  phe/keV, a result in between the one from DAMA<sup>18</sup> (6–10 phe/keV) and those from present competitors (COSINE<sup>19</sup>: 14–15.5 phe/keV; ANAIS<sup>20</sup>: 12.7–16 phe/keV). The relative energy resolution is  $\text{FWHM}/E = 13.2\%$ .

Pulse Shape Discrimination (PSD) of NaI(Tl) crystals allows studying their response to highly ionizing particles.  $\alpha$ -particles studies in Hall B permit both characterizing the PSD capabilities of the crystals, and analyzing their intrinsic backgrounds. The main handle here is the variable called Mean Time (MT), i.e. the

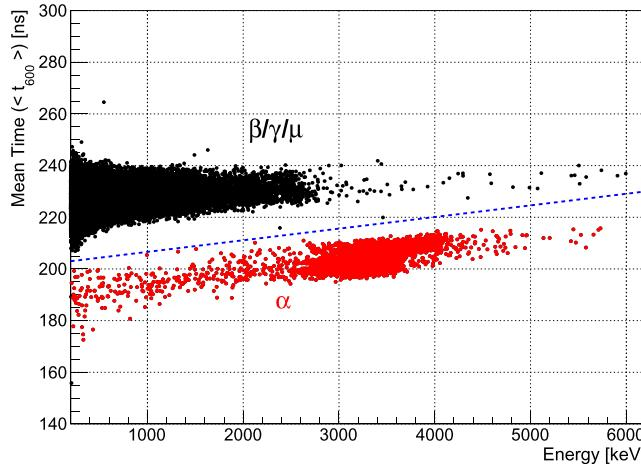


Fig. 3. Mean Time versus Energy distribution of events collected during Run1 of the LNGS Hall B set-up, crystal NaI-33. The  $\alpha$  population is clearly separated and identifiable from  $\beta$ ,  $\gamma$ -signals, and it is characterized by faster pulses.

charge-weighted duration of the pulse:

$$\text{MT} = \left( \sum_{t_i < 600 \text{ ns}} h_i t_i \right) \Bigg/ \left( \sum_{t_i < 600 \text{ ns}} h_i \right), \quad (1)$$

where  $t_i$ ,  $h_i$  are the  $i$ th time sample of a waveform and relative pulse amplitude in that bin, respectively. The Mean Time is evaluated within 600 ns from the pulse trigger.

As shown in Fig. 3, plotting this variable against the energy spectrum allows clearly identifying two separate populations, the separation increasing with energy. The  $\alpha$ -spectrum for the crystal is dominated by  $^{210}\text{Po}$ , which derives from an out-of-equilibrium contamination of  $^{210}\text{Pb}$ . By measuring the  $^{210}\text{Po}$  activity over many months (since production), a build-up trend can be derived, with an asymptotic value of  $0.51 \pm 0.02$  mBq/kg (statistical uncertainty). This activity, that corresponds to the one of  $^{210}\text{Pb}$ , is higher than SABRE target, however it is one of the lowest obtained since DAMA/LIBRA.<sup>12,13</sup> Comparing the value of the  $^{210}\text{Po}$  peak with its nominal energy of 5304 keV allows extracting the NaI(Tl) crystal Quenching Factor for  $\alpha$ 's:  $0.63 \pm 0.01$ . The spectrum used for this analysis was calibrated with a  $^{228}\text{Th}$  source.

The analysis of  $\alpha$ -particle data yields an estimation of the intrinsic crystal background related to the U,Th chains, as well. Their smaller contribution to the spectrum is evaluated from the identification of particular  $\beta - \alpha$  decay sequences, called Bismuth–Polonium (BiPo), characteristic of U and Th chains (see detailed procedure in Ref. 16). The obtained activities of daughters  $^{226}\text{Ra}$  (from the U chain) and  $^{228}\text{Th}$  (from Th chain) are  $5.9 \pm 0.6 \mu\text{Bq}/\text{kg}$  and  $1.6 \pm 0.3 \mu\text{Bq}/\text{kg}$ , respectively.

#### 4. The SABRE Proof-of-Principle

The SABRE PoP main goal is to perform a full characterization of the intrinsic and cosmogenic backgrounds of NaI(Tl) crystals at LNGS. By testing a few crystals (two-three), it should be possible to estimate the residual background rate in the ROI for DM searches. By operating the PoP, it will also be possible for the first time to study the Veto performance.

The PoP is thoroughly described in Ref. 14, and its design will be briefly summarized here, concentrating then on the commissioning procedure. The main PoP vessel is a  $\varnothing 1.3 \times 1.5$  m long low-radioactivity SS cylinder, laying horizontal. The two end-bases feature 5 flanges each, connected to isolated volumes that host PMTs for the Veto (“PMT cans”). A main flange on the top of the vessel, 60 cm in diameter, allows inserting one crystal Cu-enclosure; insertion/extraction is “dry”, i.e. independent of the opening of the main scintillator volume.

As mentioned, each crystal is coupled to two PMTs, specifically Hamamatsu R11065-20 3” PMTs, selected for their high QE ( $\sim 35\%$  at 420 nm) and low intrinsic radioactivity. The Veto is read by 10 Hamamatsu R5912-100 8” PMTs; it is filled with two tons of a solution of PC doped with PPO (2,5)-diphenyloxazole, with a concentration close to 3 g/L. The vessel inner walls are covered in Ethylene tetrafluoroethylene (ETFE), to protect the liquid scintillator from the SS, and Lumirror<sup>TM</sup> (95% reflectance for  $\lambda > 400$  nm) to improve light reflection.

The set-up lies in a SS catch-basin, and it sits on a base made of a 15 cm lead layer and a 10 cm Polyethylene (PE) sheet. Lateral inner shielding is made by PE sheets, 40 cm thick. On the top, a 2 cm SS sheet supports both a 10 cm thick PE layer below it, and the crystal insertion system: this structure is used to place/remove the detector main flange and insert/extract the crystal enclosures (see Fig. 4, left). The shielding is completed by water tanks placed on top and to the side of the PE walls, 80 and 91 cm thick, respectively (Fig. 4). All materials

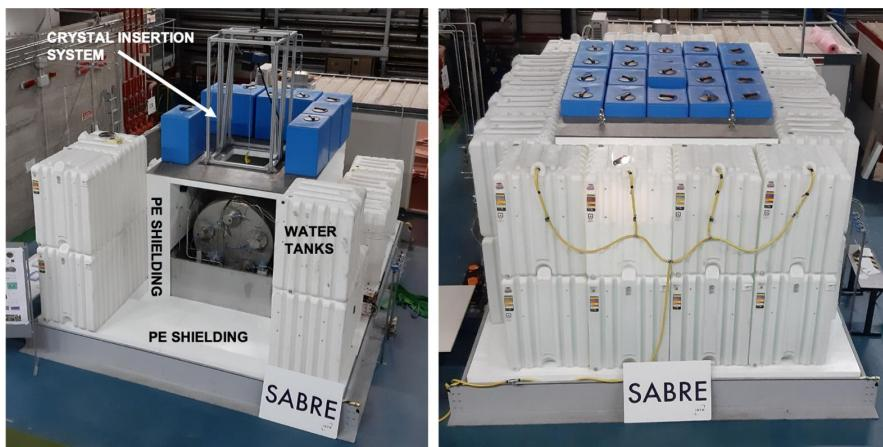


Fig. 4. Two overall views of the PoP, with the passive shielding still incomplete (left) and complete (right). The left image shows the various elements of the passive shielding and reveals the inner scintillator vessel, as well as the crystal insertion structure on the top.

were selected for their low radioactive content, according to extensive measurements with ICP-MS and High-Purity Germanium (HPGe) detectors.

#### 4.1. PoP commissioning and operation

The PoP detector commissioning started on May 25th, 2020.

The first operation was the filling of the Veto tank with  $2.23\text{ m}^3$  of de-ionized water, at an average rate  $500\text{ L/h}$  on May 26th. This operation was performed with the passive shielding partially dismounted, in order to guarantee access to the vessel. It allowed testing the filling procedure, verifying the leak tightness of the full plant, and checking the feasibility of the liquid level fine-tuning, when approaching the end of the filling process. This represented the validation of the technical and safety procedures devised for the filling with liquid scintillator.

Since the filling was completed, the slow-control system was commissioned and fully running. Veto PMTs were turned on immediately after filling, as well. Continuous data-taking allowed verifying PMT stability in time. Crystal NaI-31 was inserted on June 16th, which permitted verifying the insertion procedure and starting crystal read-out integration in the DAQ. At the same time, the circuit to flush high-purity  $\text{N}_2$  in the volume around the vessel was completed and started.

The liquid scintillator mixture (PC/PPO, called “master solution”) was prepared underground, starting on June 15th. Nine kg of PPO<sup>c</sup> were added to 300 L of PC, reaching a PPO concentration of  $27.3 \pm 0.9\text{ g/L}$ . This was measured by Gas Chromatography (GC) and double checked by gravimetric measurement by LNGS Chemistry Laboratory. The Master Solution was then purified, before insertion in SABRE, through three water extraction cycles starting on June 16th. ICP-MS measurements were performed by LNGS on samples of the Master Solution taken before and after purification, to certify the success of the procedure. On June 29th, the Master Solution, after transfer into SABRE filling tank, was diluted with more pure PC to obtain the final Liquid Scintillator. The resulting volume of 2700 L had a concentration of PPO of  $2.76\text{ g/L}$  PC, certified by GC at LNGS Chemistry Lab.

PE shielding was completed and closed on June 24th, while on June 30th the substitution of water with the liquid scintillator started. Each cycle removed about 175 L of water, replacing it with scintillator. After 13 cycles, on July 3rd, the filling operation was completed, with a total of 1970 kg of scintillator transferred.

The external water tanks were put in place and filled in the period of July 6th–14th, which basically made the detector ready for data-taking as per design. The effect of water shielding was clearly visible from a commercial NaI crystal installed inside the shielding on the PE walls, its rate of events dropping by a factor 10 during the filling operation. Data-taking with crystal NaI-31 continued until August 4th, when it was replaced with NaI-33, which also proved the feasibility of the crystal dry-insertion with the Veto running. A first data-taking campaign with NaI-33

<sup>c</sup>Emission and absorption spectra of PPO were measured in a dedicated campaign performed at Perugia University.

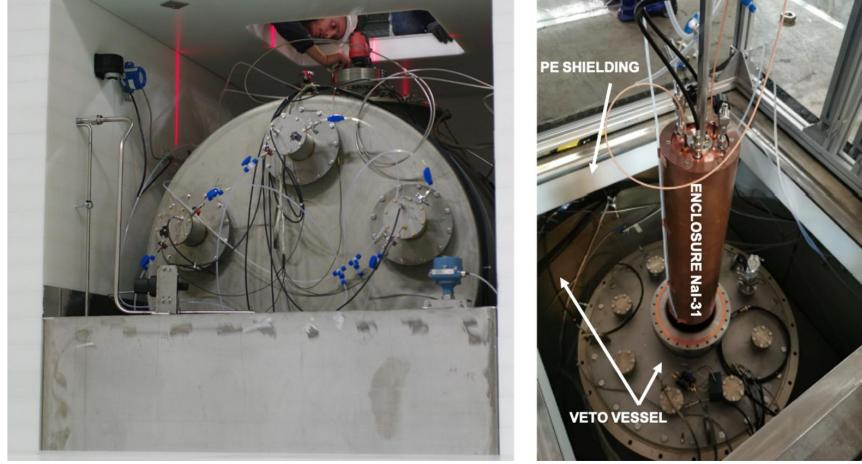


Fig. 5. Two details of the PoP installation. On the left, one end of the Veto vessel is shown during a survey, along with the “PMT cans” and their dedicated nitrogen piping. On the right, the NaI-31 crystal enclosure is being inserted in the vessel via the main top flange.

lasted around one month, ending in early September. Few images of the overall PoP and its details are shown in Figs. 4 and 5.

The activities around the PoP run are multiple: first of all, this is the very first operation of the Veto, and the chance to demonstrate its value in this kind of experiment. A review of the Veto PMTs data showed that all of them were working properly, for a total Light Yield of  $0.52 \pm 0.01$  phe/keV, i.e. more than double the Monte Carlo estimates.<sup>21</sup> This Light Yield allows for Veto operation with a 50 keV threshold, i.e. half the originally projected value. An example of Crystal-Veto coincidence event is shown in Fig. 6. First estimates of the photon mean free path yielded around 14 m, translating into an optimal performance of the reflective layers in the vessel inner walls.

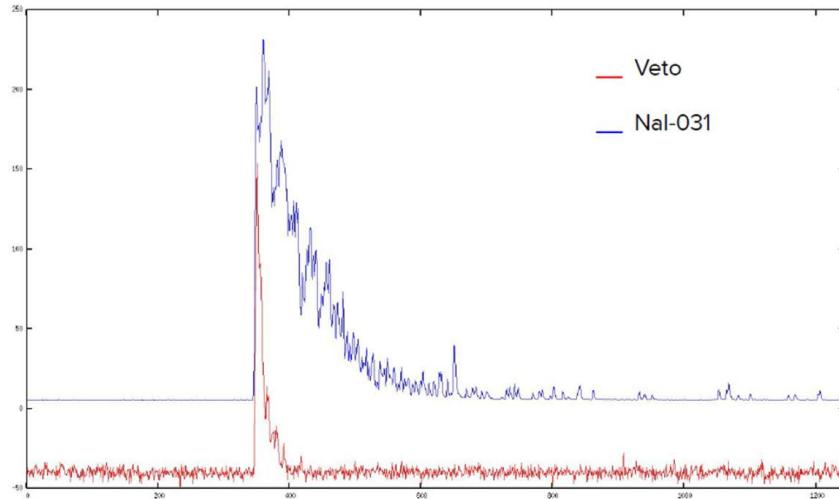


Fig. 6. (Color online) Example of coincidence event collected with the PoP and crystal NaI-31 (electron-like event). Veto-Sum signal and Crystal-Sum signal are shown, inverted, in red and blue, respectively.

The very good performance of the Veto can therefore be of extreme help for the crystal data-taking. The first phase of run with NaI-31 allows testing the so-called *Potassium Measurement Mode*, KMM, thoroughly described in Ref. 15. The higher concentration of Potassium in NaI-31 (16 ppb) should translate, according to Monte Carlo, in a rate of  $K$ -decays of around 17.5 counts/kg, accumulated in 1 month in the 2–4 keV energy region and in coincidence with high-energy deposits in the Veto. This yields enough statistics to test this measurement mode, which entails the coincidence between Veto and Crystal triggers. While the analysis is still under way, we are confident that we will be able to make a statement concerning the potassium background of the crystals with this technique.

In the end, however, the actual full validation of the SABRE concept will come from the data collected with NaI-33. This will entail fully characterizing both intrinsic and environmental backgrounds, i.e. producing a full background model and making a statement about the actual energy detection threshold that can be achieved with SABRE. This analysis represents in many ways the real first step towards the realization of a full-scale SABRE detector, and it will be the focus of a future publication.

## 5. Outlook

Despite the COVID-19 pandemic, the activities of the SABRE experiment saw a turning point in 2020. The characterization of the first very-high-purity crystal, NaI-33, was completed with a dedicated set-up in Hall B of LNGS: a dedicated paper reporting the results of such work was published in 2021.<sup>16</sup> The crystal was later inserted in the PoP detector, in LNGS Hall C, which was commissioned in the summer of 2020.

The commissioning of the PoP was an important milestone of the project, as it first validated all the technical procedures related to liquid scintillator handling and purification. Then, most importantly, it was possible to perform data-taking with a set-up fully representing the SABRE design, which alone can yield meaningful hints about the detection energy threshold the program will actually achieve. The PoP first housed the NaI-31 crystal, a less pure predecessor to NaI-33, with high enough potassium contamination to try and perform a search for the events produced by  $^{40}\text{K}$  decays. Later, as mentioned, crystal NaI-33 was inserted. At the same time, a dedicated characterization of the Veto detector, including Light Yield and energy resolution, was performed. Preliminary results from the Veto suggest 100% functionality of the PMTs and very high reflectivity of the inner vessel. All the collected data are presently being analyzed and will be the focus of a dedicated paper.

The future holds several new challenges for the collaboration, nonetheless. Despite the excellent results achieved with crystal NaI-33, new advanced solutions are already under development to obtain even cleaner crystals: these go from in-house powder production and growth at PU, to the use of *Zone Refining* (ZR<sup>22</sup>),

which should further reduce intrinsic contamination. The goal here is to produce a new crystal (NaI-34) with such techniques in 2021.

At the same time, the PoP commissioning demonstrated that the next step is within reach. SABRE-South activities are proceeding quite smoothly and the hardware construction is well advanced: therefore, it is reasonable to assume that the installation and commissioning of that detector should follow without issues. On the other hand, the final proposal for the Northern full-scale experiment will be driven by results obtained with the summer 2020 PoP run.

## Acknowledgments

The SABRE program is supported by funding from INFN (Italy), NSF (USA) and ARC (AUS). We thank the Director and staff of LNGS for their support, in particular G. Bucciarelli, M. D’Incecco, C. Ianni, M. Laubenstein, P. Martella, M. Orsini, G. Panella, C. Zarra (INFN LNGS), for their contribution on the realization of the SABRE PoP set-up. Finally, we would like to acknowledge the fundamental contribution of S. Nisi, F. Marchegiani, L. Ioannucci (INFN LNGS) and F. Ortica (Perugia University) to the characterization of the liquid scintillator used in the SABRE PoP.

## References

1. G. Bertone and D. Hooper, *Rev. Mod. Phys.* **90**, 045002 (2018).
2. G. Arcadi *et al.*, *Eur. Phys. J. C* **78**, 203 (2018).
3. K. Freese, J. Frieman and A. Gould, *Phys. Rev. D* **37**, 3388 (1988).
4. DAMA Collab. (R. Bernabei *et al.*), *Eur. Phys. J. C* **73**, 2648 (2013).
5. DAMA Collab. (R. Bernabei *et al.*), *Nucl. Phys. At. Energy* **19**, 307 (2019).
6. XMASS Collab. (M. Kobayashi *et al.*), *Phys. Lett. B* **795**, 308 (2019).
7. XENON Collab. (E. Aprile *et al.*), *Phys. Rev. Lett.* **121**, 111302 (2018).
8. DarkSide Collab. (P. Agnes *et al.*), *Phys. Rev. Lett.* **121**, 081307 (2018).
9. CRESST Collab. (A. H. Abdelhameed *et al.*), *Phys. Rev. D* **100**, 102002 (2019).
10. COSINE-100 Collab. (P. Adhikari *et al.*), *Nature* **7734**, 83 (2018).
11. I. Coarasa *et al.*, *Eur. Phys. J. C* **79**, 233 (2019).
12. COSINE-100 Collab. (G. Adhikari *et al.*), arXiv:2101.11377 [astro-ph.IM].
13. J. Amaré *et al.*, *Eur. Phys. J. C* **79**, 412 (2019).
14. SABRE Collab. (M. Antonello *et al.*), *Eur. Phys. J. C* **79**, 363 (2019).
15. SABRE Collab. (M. Antonello *et al.*), *Astropart. Phys.* **106**, 1 (2019).
16. SABRE Collab. (M. Antonello *et al.*), *Eur. Phys. J. C* **81**, 299 (2021).
17. J. Diemand and B. Moore, *Adv. Sci. Lett.* **4**, 297 (2011).
18. R. Bernabei *et al.*, *J. Instrum.* **7**, P03009 (2012).
19. COSINE-100 Collab. (G. Adhikari *et al.*), *Eur. Phys. J. C* **78**, 107 (2018).
20. J. Amaré *et al.*, *Eur. Phys. J. C* **79**, 228 (2019).
21. E. Shields, SABRE: A search for dark matter and a test of the DAMA/LIBRA annual-modulation result using thallium-doped sodium-iodide scintillation detectors, Ph.D. thesis, Princeton University (2015).
22. W. G. Pfann, *JOM* **4**, 747 (1952).